

1-1-2014

# Rotational Quenching of H<sub>2</sub>O by He: Mixed Quantum/Classical Theory and Comparison with Quantum Results

Mikhail V. Ivanov  
*Marquette University*

Marie-Lise Dubernet  
*PSL Research University*

Dmitri Babikov  
*Marquette University, dmitri.babikov@marquette.edu*

# Rotational quenching of H<sub>2</sub>O by He: Mixed quantum/classical theory and comparison with quantum results

Mikhail Ivanov,<sup>1,2,a)</sup> Marie-Lise Dubernet,<sup>1</sup> and Dmitri Babikov<sup>2,b)</sup>

<sup>1</sup>*PSL Research University, Observatoire de Paris, Sorbonne Universités, UPMC Univ Paris 06, ENS, UCP, CNRS, UMR8112, LERMA, 5 Place Janssen, 92195 Meudon, France*

<sup>2</sup>*Department of Chemistry, Marquette University, Milwaukee, Wisconsin 53201-1881, USA*

(Received 8 January 2014; accepted 6 March 2014; published online 2 April 2014)

The mixed quantum/classical theory (MQCT) formulated in the space-fixed reference frame is used to compute quenching cross sections of several rotationally excited states of water molecule by impact of He atom in a broad range of collision energies, and is tested against the full-quantum calculations on the same potential energy surface. In current implementation of MQCT method, there are two major sources of errors: one affects results at energies below 10 cm<sup>-1</sup>, while the other shows up at energies above 500 cm<sup>-1</sup>. Namely, when the collision energy  $E$  is below the state-to-state transition energy  $\Delta E$  the MQCT method becomes less accurate due to its intrinsic classical approximation, although employment of the average-velocity principle (scaling of collision energy in order to satisfy microscopic reversibility) helps dramatically. At higher energies, MQCT is expected to be accurate but in current implementation, in order to make calculations computationally affordable, we had to cut off the basis set size. This can be avoided by using a more efficient body-fixed formulation of MQCT. Overall, the errors of MQCT method are within 20% of the full-quantum results almost everywhere through four-orders-of-magnitude range of collision energies, except near resonances, where the errors are somewhat larger. © 2014 AIP Publishing LLC. [<http://dx.doi.org/10.1063/1.4868715>]

## I. INTRODUCTION

The current paper aims at investigating the use of a mixed quantum/classical theory (MQCT) for rotational quenching of a rigid asymmetric top molecule by an atom, applying this method to H<sub>2</sub>O + He system, and comparing results against the full-quantum close-coupling (CC) calculations.

Development of the mixed quantum/classical theories of inelastic scattering dates back to 1960s and 1970s, when the focus was mostly on electronic transitions in atom + atom collisions.<sup>1</sup> The work of McCann and Flannery<sup>2-4</sup> in 1970s extended these ideas onto rotational and vibrational transitions in a diatomic molecule collided with an atom, which was then revisited and further developed by Billing in the 1980s and 1990s.<sup>5,6</sup> In such mixed quantum/classical methods, the scattering motion of the atom with respect to the molecule is always treated classically, but there are two options for treatment of the internal ro-vibrational motion of the molecule.

One option is to restrict quantum mechanical description to vibrational degrees of freedom only, treating molecular rotation classically. This approach received most of attention and was applied to several molecular systems such as diatomic + atom, triatomic + atom, and diatomic + diatomic by Billing and his numerous collaborators<sup>5-10</sup> and later by Light.<sup>11</sup> In recent years, it was re-introduced by Babikov

and collaborators<sup>12-17</sup> and tested against the full-quantum calculations in a broad range of scattering energies.<sup>18,19</sup>

Another option is to treat rotational motion of the molecule quantum mechanically, either keeping the vibrational motion frozen (which corresponds to the rigid rotor) or treating it also quantum mechanically, in which case all the internal molecular degrees of freedom are described coherently. Surprisingly, this approach received very little attention. Billing<sup>20-22</sup> applied it to the simplest system – rotational quenching of H<sub>2</sub>( $j = 2$ ) by He impact, and compared his results vs. full-quantum calculations available at that time (at two values of scattering energies only) and experimental data. Of course, comparison with experiment is the ultimate goal, but there may be other sources of disagreement between theory and experiment, besides approximations inherent to theoretical approach. It would certainly be desirable to see how results of this method would compare to results of full-quantum calculations on the same potential energy surface (PES) in a broad range of collision energies. To the best of our knowledge such benchmark study has not been carried out by Billing<sup>20-22</sup> or anyone else. Furthermore, it appears that Billing<sup>20-22</sup> used only a simplified version of MQCT, known as coupled-states (CS) approximation.

Recently, Semenov and Babikov<sup>23</sup> published an improved fully coupled version of MQCT for ro-vibrationally inelastic scattering in both space-fixed (SF) and body-fixed (BF) reference frames. This development enabled calculations of rotational quenching and excitation in a broad range of collision energies in two real diatomic + atom systems,<sup>24,25</sup> one of which had all light atoms, H<sub>2</sub> + He, while the other

<sup>a)</sup>Permanent address: Institute of Precambrian Geology and Geochronology, Russian Academy of Sciences, nab. Makarova 2, 199034 St. Petersburg, Russia.

<sup>b)</sup>Author to whom correspondence should be addressed. Electronic mail: [dmitri.babikov@mu.edu](mailto:dmitri.babikov@mu.edu)

had all reasonably heavy atoms,  $N_2 + Na$ . Elastic and inelastic, integral and differential (over scattering angle) cross sections were computed and compared to full-quantum calculations. Several low-lying and some highly excited rotational states were tried. Both the fully coupled and the approximate CS-version of MQCT were tested.<sup>25</sup> These extensive benchmark studies showed that MQCT is a promising approach to computational studies of rotationally inelastic scattering.

The next logical step, and the goal of this paper, is to expand the rotationally inelastic version of MQCT in order to be able to describe quenching of a rigid asymmetric top rotor by an atom, apply such theory to a real triatomic molecule, and compare results of MQCT against the full quantum calculations using the same PES, in a broad range of collision energies. This has never been done in the past and is not a trivial problem, since both theory development and extensive calculations are needed. MQCT theory is simpler to formulate in the SF reference frame, and we pursue this approach here.

## II. THEORY

In a mixed quantum/classical approach, the basic assumption is the existence over the inelastic coupling region of a common mean trajectory  $\vec{R}(t)$  for the relative motion, governed by an appropriate average potential.<sup>6</sup> Within this picture the relative kinetic operator may be omitted from the quantum Hamiltonian and be replaced by a time-dependent interaction potential  $V(\vec{R}(t), \mathbf{\Omega})$  where  $\mathbf{\Omega}$  is a collective notation for the internal rotational degrees of freedom of the molecule, i.e., the Euler angles  $(\alpha, \beta, \gamma)$  that rotate the space-fixed axis to an axis system fixed in the frame of the molecule. For the water molecule, the molecule-fixed axis  $z$  is along the symmetry axis of the water molecule, and the plane  $xz$  is a plane of symmetry. A general orientation  $(\alpha, \beta, \gamma)$  is produced by rotating the molecule-fixed axis system, beginning at  $(0,0,0)$ , by an angle  $\alpha$  about the molecule-fixed axis  $z$ , followed by a rotation  $\beta$  about the molecule-fixed axis  $y$ , and then another rotation  $\gamma$  about the molecule-fixed axis  $z$ .

Hence, the time-dependent Schrödinger equation governing the evolution of time-dependent rotational wave function is

$$i\hbar \frac{d\psi(\mathbf{\Omega}, t)}{dt} = [\hat{H}_{rot} + V(\vec{R}(t), \mathbf{\Omega})]\psi(\mathbf{\Omega}, t). \quad (1)$$

The time-dependent rotational wave function is expanded over the basis set of unperturbed rotational eigenstates  $\phi_{j\tau m}(\mathbf{\Omega})$  that correspond to the eigenvalues  $E_{j\tau}$

$$\psi(\mathbf{\Omega}, t) = \sum_{j\tau m} c_{j\tau m}(t) \phi_{j\tau m}(\mathbf{\Omega}) \exp(-iE_{j\tau}t/\hbar), \quad (2)$$

where  $j$  is the rotational quantum number of the asymmetric top molecule,  $\tau$  is the pseudo-quantum number that varies between  $-j$  and  $j$  (alternatively, we may use the pseudo-quantum numbers  $k_a, k_c$  with the correspondence  $\tau = k_a - k_c$ ), and  $m$  the eigenvalue of the  $\hat{J}_Z$  operator where  $Z$  is the axis of space-fixed reference frame. The unperturbed asymmetric top eigenstates  $\phi_{j\tau m}$  are expressed in terms of symmetric top eigenstates as

$$\phi_{j\tau m}(\alpha, \beta, \gamma) = \sum_k a_{\tau k}^j ((2j+1)/8\pi^2)^{1/2} \mathcal{D}_{km}^j(\alpha, \beta, \gamma), \quad (3)$$

where the  $\mathcal{D}_{km}^j(\alpha, \beta, \gamma)$  are Wigner rotation functions defined according to conventions of Silver<sup>26</sup> with  $k$  the projection of  $\hat{J}$  on the molecule-fixed  $z$ -axis. The coefficients  $a_{\tau k}^j$  and the eigenvalues  $E_{j\tau}$  are obtained by diagonalizing the Hamiltonian of the unperturbed asymmetric rotor

$$\hat{H}_{rot} = (2I_x)^{-1} \mathcal{J}_x^2 + (2I_y)^{-1} \mathcal{J}_y^2 + (2I_z)^{-1} \mathcal{J}_z^2, \quad (4)$$

where  $I_\alpha$  are the principal moments of inertia in the molecule-fixed axis and  $\mathcal{J}_\alpha^2$  the angular momentum operators about the corresponding axes.<sup>27</sup>

Substitution of Eq. (2) into Eq. (1) leads to a system of coupled equations for the time dependent coefficients  $c_{j\tau m}(t)$

$$i\hbar \frac{dc_{j\tau m}(t)}{dt} = \sum_{j'\tau'm'} c_{j'\tau'm'}(t) \exp(-i(E_{j'\tau'} - E_{j\tau})t/\hbar) \times \langle \phi_{j\tau m}(\mathbf{\Omega}) | V(\vec{R}(t), \mathbf{\Omega}) | \phi_{j'\tau'm'}(\mathbf{\Omega}) \rangle. \quad (5)$$

In the space-fixed reference frame, the relative vector joining the center of mass of the partners,  $\vec{R}(t)$  can be expressed either using polar coordinates  $(R(t), \Theta(t), \Phi(t))$  or using Cartesian coordinates  $(X(t), Y(t), Z(t))$ . The relative Cartesian coordinates correspond to  $\mathbf{Q}(t) = \mathbf{q}_{H_2O}(t) - \mathbf{q}_{He}(t)$  with  $\mathbf{q}_\alpha(t)$  the Cartesian coordinates of the center of mass of the partners in space-fixed reference frame.

The mixed quantum/classical method uses the Ehrenfest theorem with additional approximations in order to calculate the trajectory  $\vec{R}(t)$ . The Ehrenfest theorem<sup>28</sup> gives the time evolution of the average of the coordinates  $q$  and of the conjugate momenta  $p$  of a quantum system. If we consider  $q_1, q_2, \dots, p_1, p_2, \dots$  and the Hamiltonian of the quantum system is  $\mathcal{H}(q_1, q_2, \dots; p_1, p_2, \dots)$ , the time evolution of the average  $\langle q_i \rangle$  and  $\langle p_i \rangle$  is given by

$$i\hbar \frac{d}{dt} \langle q_i \rangle = \left\langle \frac{\partial \mathcal{H}}{\partial p_i} \right\rangle, \quad (6)$$

$$i\hbar \frac{d}{dt} \langle p_j \rangle = - \left\langle \frac{\partial \mathcal{H}}{\partial q_j} \right\rangle, \quad (7)$$

where the average is taken over the wave function  $\Psi$  that satisfy the time dependent Schrödinger equation involving  $\mathcal{H}$ .

For the problem at hand, the total Hamiltonian describing our system depends upon the internal angular coordinates  $\mathbf{\Omega}$ , on the centers of mass coordinates  $\mathbf{q}_\alpha$ , on their conjugate momenta  $\mathbf{p}_\Omega, \mathbf{p}_\alpha$  and is given by

$$\mathcal{H}_{tot} = \hat{T} + \hat{H}_{rot} + V(\vec{R}(t), \mathbf{\Omega}), \quad (8)$$

where  $\hat{T}$  is the kinetic energy operator for translational motion of the collision partners

$$\hat{T} = \frac{P_{H_2O}^2}{2m_{H_2O}} + \frac{P_{He}^2}{2m_{He}}. \quad (9)$$

The total wave function satisfying the time-dependent Schrödinger equation involving  $\mathcal{H}_{tot}$  can be expanded on products  $\psi(\mathbf{\Omega}, t)\Gamma$ , where  $\Gamma$  is the time dependent translational wave function. In the classical limit, it is assumed that

the wave packet  $\Gamma$  is localized enough so that in Eqs. (6) and (7) we can replace  $\langle q \rangle$  and  $\langle p \rangle$  by the classical positions and momenta  $q_{cl}$  and  $p_{cl}$  of the centers of mass of the partners. This is possible if we replace in the second half of Eqs. (6) and (7) the average

$$\langle \Gamma | \frac{\partial \mathcal{H}_{tot}}{\partial p_i}(\mathbf{\Omega}, \mathbf{p}_{\Omega}; q_i, p_i) | \Gamma \rangle, \quad (10)$$

by

$$\begin{aligned} & \frac{\partial \mathcal{H}_{tot}}{\partial p_i}(\mathbf{\Omega}, \mathbf{p}_{\Omega}; \langle q_i \rangle, \langle p_i \rangle) \\ &= \frac{\partial \mathcal{H}_{tot}}{\partial p_i}(\mathbf{\Omega}, \mathbf{p}_{\Omega}; (q_i)_{cl}, (p_i)_{cl}). \end{aligned} \quad (11)$$

Here  $i = 1, 6$ . Hence, in the classical limit Eq. (6) becomes for each center of mass of the partners

$$i\hbar \frac{d}{dt} q_i = p_i / m_{\alpha} \quad (12)$$

with  $m_{\alpha}$  being the mass of the partner; and Eq. (7) becomes

$$\begin{aligned} i\hbar \frac{d}{dt} p_j &= -\frac{\partial}{\partial q_j} \langle \phi_{j\tau m}(\mathbf{\Omega}) | V(\vec{R}(t), \mathbf{\Omega}) | \phi_{j'\tau' m'}(\mathbf{\Omega}) \rangle \\ &= -\frac{\partial}{\partial q_j} \langle \phi_{j\tau m}(\mathbf{\Omega}) | V(q_1, q_2, \dots, \mathbf{\Omega}) | \phi_{j'\tau' m'}(\mathbf{\Omega}) \rangle. \end{aligned} \quad (13)$$

The propagation of Eqs (5), (12), and (13) will provide the coefficients  $c_{j\tau m}(t = \infty)$  that will allow to calculate the transition probabilities between rotational energy levels. Energy of the final rotational wave packet is given by

$$\langle E \rangle = \sum_{j'\tau' m'} c_{j'\tau' m'}^2(t = \infty) E_{j'\tau'}. \quad (14)$$

Conservation of energy can be expressed as:  $E_{in} + E_{j\tau} = E_{out} + \langle E \rangle$ , where “in” and “out” label the kinetic energy of classical trajectory before and after collision, the initial state is unprimed, final states are primed. Strictly speaking, the sum in Eq. (14) contains all states of the basis set, including states of the channels energetically closed at given collision energy. Indeed, in the mixed quantum/classical approach the total energy is conserved only on average and, if the transition probability is small, even a highly excited energetically closed channel can participate in the process. Usually, transitions to such energetically closed channels are negligibly weak and cause no problem,<sup>24,25</sup> but here we found that at low collision energies (roughly  $E < \Delta E/2$ , where  $\Delta E = E_{j'\tau'} - E_{j\tau}$ ) the intensity of transitions to closed channels grows catastrophically, which is also accompanied by intense transitions to the low-lying states, due to conservation of the total average energy. We saw that at low collision energies this internal redistribution of energy within the wave packet can be many times larger than the energy exchange between the molecule and the colliding atom, which affects strongly the values of quenching cross sections, and is unphysical. In order to eliminate this behavior, one can reduce the size of the basis set to the open channels only (at given collision energy), using the condition  $E_{j'\tau'} < E_{in} + E_{j\tau}$ . This is different from the

full-quantum calculations, where some closed channels were included in order to ensure convergence.

For calculations at high collision energies, the size of the basis set can be reduced further in order to ease calculations. This is an issue of convergence (with respect to the basis set size), and it should be checked by repeating calculations with different basis set sizes. We used the following condition:  $E_{j'\tau'} < E_{max} + E_{j\tau}$ , where the value of cut-off energy was chosen equal to  $E_{max} = 500 \text{ cm}^{-1}$ . At collision energies  $E_{in} > E_{max}$  such cut-off procedure removes some highly excited states that formally become open, but in practice remain weakly populated. In order to check the effect of this cut-off, we carried out additional calculations with  $E_{max} = 1000 \text{ cm}^{-1}$  for one transition, from state  $1_{1,1}$  to state  $0_{0,0}$ . The difference was slightly below 5%, and it was decided to use  $E_{max} = 500 \text{ cm}^{-1}$  for all processes studied here.

Thus, calculations at low collision energies involved 4, 6, and 9 states in the basis for the initial states  $1_{1,1}$ ,  $1_{1,0}$ , and  $2_{0,2}$ , respectively. At energies  $E = 500 \text{ cm}^{-1}$  calculations involved 131, 137, and 144 states in the basis, while at energies  $E = 1000 \text{ cm}^{-1}$  calculations involved 348, 356, and 365 states in the basis, for the initial states  $1_{1,1}$ ,  $1_{1,0}$ , and  $2_{0,2}$ , respectively.

An efficient Monte Carlo procedure for sampling the initial conditions for classical degrees-of-freedom was described in detail in a recent paper by Semenov and Babikov<sup>23</sup> (see Fig. 1 and Eqs. (12)–(15) there). Here, for calculations in the SF reference frame, the center of mass of water molecule at the initial moment of time was placed at the origin, while the initial position of He atom was sampled randomly and uniformly in a plane placed at a distance of  $20 a_0$  from the origin. Note that in MQCT calculations the sampling over impact parameter replaces summation over orbital quantum number

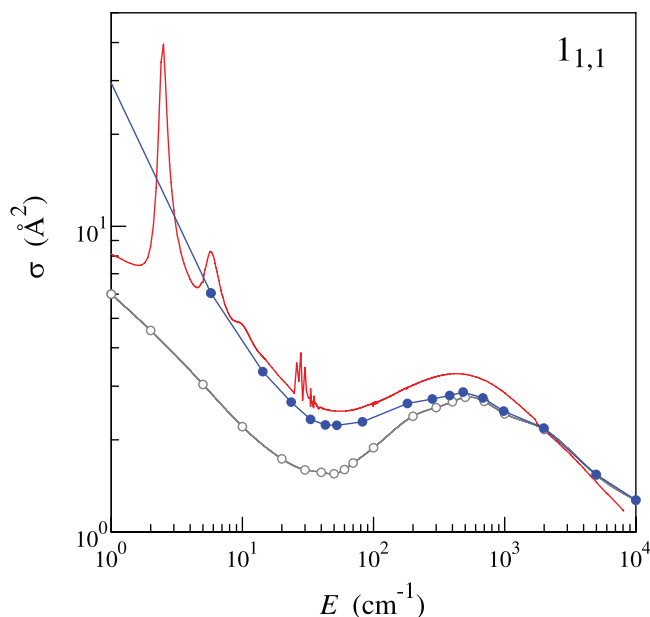


FIG. 1. Energy dependence of quenching cross section for the first excited state  $1_{1,1}$  of para-water. Blue symbols (connected by straight lines) represent final results of MQCT calculations, obtained using the average velocity approach. Red line gives results of the full-quantum calculations. Grey symbols represent the raw or unscaled results of MQCT.

(used in the full-quantum approach).<sup>23</sup> In this work, the maximum value of impact parameter was determined by convergence studies, for each value of collision energy separately. It varied from  $b_{max} = 8 a_0$  used for  $E > 1000 \text{ cm}^{-1}$  to  $b_{max} = 20 a_0$  used for  $E < 10 \text{ cm}^{-1}$ .

### III. MATRIX ELEMENTS OF THE POTENTIAL ENERGY SURFACE

Both in the semi-classical and the quantum calculations, we use the *ab initio* SAPT PES of Patkowski *et al.*<sup>29</sup> that has been tested by Yang *et al.*<sup>30,31</sup> to obtain new rate coefficients for the rotational excitation of lowest 10 levels of ortho/para- $\text{H}_2\text{O}$  by He.<sup>30-32</sup> This PES is calculated in relative coordinates with respect to the molecular fixed coordinate system described in Sec. II. Indeed, as described by Patkowski *et al.*,<sup>29</sup> the water molecule lay in the molecular  $xz$  plane, with oxygen on the positive half of the molecular  $z$  axis. The position of helium is expressed in spherical polar coordinates  $(R, \theta, \phi)$ , so that  $\theta = 0$  for He on the oxygen side of the water  $C_{2v}$  axis, and  $\phi = 0$  when all four atoms are coplanar.

Within this molecule-fixed coordinate system the PES is usually expanded in spherical harmonics as

$$V^{MF}(R, \theta, \phi) = \sum_{p_1 q_1} v_{p_1 q_1}(R) [Y_{p_1 q_1}(\theta, \phi) + (-)^{q_1} Y_{p_1 -q_1}(\theta, \phi)], \quad 0 \leq q_1 \leq p_1. \quad (15)$$

Nevertheless, both the MQCT and the full-quantum calculations require a potential energy surface written in space-fixed coordinates. Similar to the expression of Phillips *et al.*,<sup>27</sup> reduced to a rigid asymmetric top + atom system, the PES is therefore expanded in space fixed coordinates as

$$V^{SF}(R, \Theta, \Phi, \alpha, \beta, \gamma) = \sum_{p_1 q_1} v_{p_1 q_1}(R) T_{p_1 q_1}(\Theta, \Phi, \alpha, \beta, \gamma), \quad 0 \leq q_1 \leq p_1, \quad (16)$$

with

$$T_{p_1 q_1}(\Theta, \Phi, \alpha, \beta, \gamma) = \frac{1}{1 + \delta_{q_1, 0}} \sum_{r_1} Y_{p_1 r_1}(\Theta, \Phi) [\mathcal{D}_{q_1 r_1}^{p_1}(\alpha, \beta, \gamma) + (-)^{q_1} \mathcal{D}_{-q_1 r_1}^{p_1}(\alpha, \beta, \gamma)], \quad (17)$$

where  $-q_1 \leq r_1 \leq p_1$  and where the molecular fixed expression corresponds to  $\alpha = 0, \beta = 0, \gamma = 0$  with  $\Theta, \Phi$  becoming  $\theta, \phi$  (the collision direction).

The coupling term  $\langle \phi_{j\tau m}(\mathbf{\Omega}) | V(\vec{R}(t), \mathbf{\Omega}) | \phi_{j'\tau' m'}(\mathbf{\Omega}) \rangle$  of Eq. (5) is then given by the matrix elements of  $V^{SF}(R, \Theta, \Phi, \alpha, \beta, \gamma)$  over asymmetric top eigenstates (Eq. (3))

$$\begin{aligned} & \langle \phi_{j\tau m}(\alpha, \beta, \gamma) | V^{SF} | \phi_{j'\tau' m'}(\alpha, \beta, \gamma) \rangle \\ &= \frac{1}{1 + \delta_{q_1, 0}} \sum_{p_1 q_1} v_{p_1 q_1}(R) \sum_{kk'} a_{\tau k}^j a_{\tau' k'}^{j'} [j][j'] (-)^{k-m} \\ & \times \left[ \begin{pmatrix} j & p_1 & j' \\ -k & q_1 & k' \end{pmatrix} + (-)^{q_1} \begin{pmatrix} j & p_1 & j' \\ -k & -q_1 & k' \end{pmatrix} \right] \\ & \times \sum_{r_1} Y_{p_1 r_1}(\Theta, \Phi) \begin{pmatrix} j & p_1 & j' \\ -m & r_1 & m' \end{pmatrix}, \quad (18) \end{aligned}$$

where  $[j] = (2j + 1)^{1/2}$  and  $R, \Theta, \Phi$  are time-dependent quantities.

For CC calculations, the potential matrix elements are taken over the total wave function usually expanded over basis functions which are eigenfunctions of the total angular momentum  $J$  such as

$$\begin{aligned} & \Psi_{j\tau l}^{JM}(\Theta, \Phi, \alpha, \beta, \gamma) \\ &= \sum_{mm_l} \langle j m l m_l | J M \rangle \phi_{j\tau m}(\alpha, \beta, \gamma) Y_{l m_l}(\Theta, \Phi), \quad (19) \end{aligned}$$

where  $\langle j m l m_l | J M \rangle$  is a Clebch-Gordan coefficient, and are diagonal in  $J$  and independent of  $M$  (space-fixed projection of  $\hat{J}$ ). These matrix elements can be obtained by reducing Eq. (11) of Phillips *et al.*,<sup>27</sup> to an asymmetric top-atom system and are given by

$$\begin{aligned} \langle \Psi_{j\tau l}^{JM} | V^{SF} | \Psi_{j'\tau' l'}^{JM} \rangle &= \frac{1}{\sqrt{4\pi}(1 + \delta_{q_1, 0})} \sum_{p_1 q_1} v_{p_1 q_1}(R) \sum_{kk'} a_{\tau k}^j a_{\tau' k'}^{j'} [j][j'] [l][l'] [p_1] (-)^{J-j'-j+k} \\ & \times \left[ \begin{pmatrix} j & p_1 & j' \\ -k & q_1 & k' \end{pmatrix} + (-)^{q_1} \begin{pmatrix} j & p_1 & j' \\ -k & -q_1 & k' \end{pmatrix} \right] \begin{pmatrix} l & l' & p_1 \\ 0 & 0 & 0 \end{pmatrix} \left\{ \begin{matrix} l & l' & p_1 \\ j' & j & J \end{matrix} \right\}, \quad (20) \end{aligned}$$

where  $[l] = (2l + 1)^{1/2}$ . This expression is compatible with Eq. (26) of Green.<sup>33</sup>

### IV. CLOSE COUPLING QUANTUM CALCULATIONS

The full-quantum scattering calculations were performed using modified versions of both the sequential and parallel versions of the MOLSCAT code<sup>34,35</sup> using the Airy propagator.<sup>36</sup> The water molecule is described by a version of

the effective Hamiltonian of Kyro,<sup>37</sup> compatible with the symmetries of the PES. We use the molecular constants from Table I of Kyro<sup>37</sup> and our calculated rotational levels of  $\text{H}_2^{16}\text{O}$  are identical to those of Green.<sup>38</sup> Close coupling calculations are carried out up to collision energy  $8000 \text{ cm}^{-1}$ . The rotational basis set includes, in addition to open channels, 10 closed channels for all total energies up to  $2000 \text{ cm}^{-1}$ , and is reduced to 5 closed channels for higher energies. State-to-state transition cross sections were converged to better than 1%. Our

rate coefficients for quenching can be compared to those of Yang *et al.*<sup>30,31</sup> obtained with roughly the same methodology and using the same potential energy surface. For example, for transition from  $1_{1,1}$  to  $0_{0,0}$  in the temperature range 5–800 K the difference is below or about 1%.<sup>30–32</sup>

## V. ANALYSIS AND DISCUSSIONS

In Fig. 1, we report results for quenching of the first excited state of para-water  $1_{1,1}$  onto the ground rotational state  $0_{0,0}$  ( $\Delta E = -37.14$  cm<sup>-1</sup>). The value of quenching cross section is presented as a function of collision energy in a broad range (note that logarithmic scale is used for both axes). Red line gives results of the full-quantum (CC) calculations, used here as a benchmark. Two sets of MQCT data are presented: Gray symbols/line give the *raw* MQCT data, where the value of cross section is plotted as a function of trajectory energy in computer simulations. Blue symbols/line give the *final* MQCT results, scaled using the average-velocity principle<sup>6,19</sup> in order to incorporate microscopic reversibility. Overall, these final MQCT results are in reasonable agreement with full-quantum results in a broad range of collision energies, from 1 cm<sup>-1</sup> to 10 000 cm<sup>-1</sup>. In this energy interval, the dependence of quenching cross section exhibits pronounced oscillations, passing through the minimum near 55 cm<sup>-1</sup> and the maximum near 500 cm<sup>-1</sup>. Results of MQCT calculations reproduce this behavior really well. Even at energies below 10 cm<sup>-1</sup>, where the full-quantum cross section exhibits broad scattering resonances, the results of MQCT calculations still follow the benchmark data, on average.

In Fig. 2, we report results for quenching of the first excited state of ortho-water  $1_{1,0}$  onto its ground rotational state  $1_{0,1}$  ( $\Delta E = -18.60$  cm<sup>-1</sup>), in the same broad range of collision energies. Here, the agreement of MQCT results with full-quantum benchmark data is even better, particularly in the

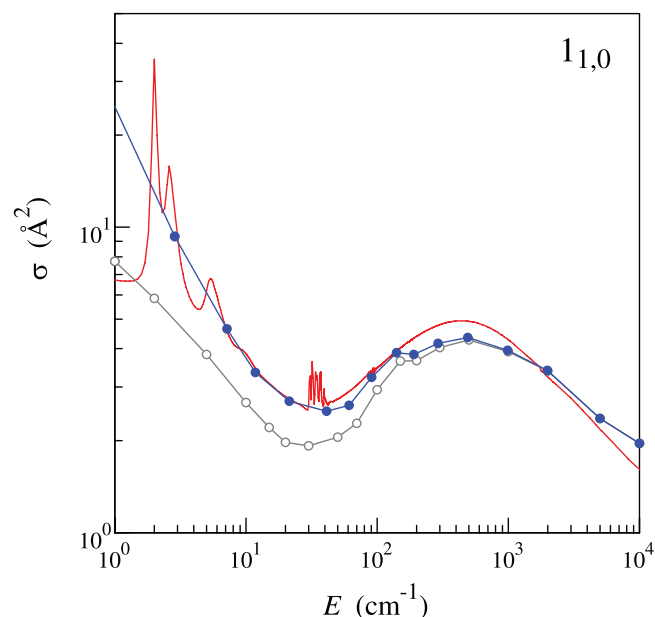


FIG. 2. Same as in Fig. 1, but for quenching of the first excited state  $1_{1,0}$  of ortho-water.

intermediate energy range, from 5 cm<sup>-1</sup> to 150 cm<sup>-1</sup>. At energies below 5 cm<sup>-1</sup> we see that, again, MQCT cross section exhibits behavior close to average over broad scattering resonances. Overall, the energy dependence of cross section, including oscillations, the minimum and the maximum, is well reproduced by the average-velocity (scaled) MQCT consistent with microscopic reversibility, and not so well by the *raw* trajectory data.

In Fig. 3, we report results for quenching of the second excited state of para-water  $2_{0,2}$ . For this state, there are two quenching pathways: onto the ground rotational state  $0_{0,0}$  directly ( $\Delta E = -70.13$  cm<sup>-1</sup>) and through the first excited para-state  $1_{1,1}$  ( $\Delta E = -32.97$  cm<sup>-1</sup>). First of these processes is 3–4 times less intense than the second one, and cross sections for both are presented in Fig. 3. Performance of MQCT method is similar to what we saw in Figs. 1 and 2. The value of cross section slightly oscillates (less than in Figs. 1 and 2) through the energy range from 1 cm<sup>-1</sup> to 10 000 cm<sup>-1</sup>, and this behavior is captured by MQCT. The effect of broad scattering resonances at energies below 10 cm<sup>-1</sup> is reproduced on average rather well. Full-quantum calculations also show some very narrow scattering resonances at higher energies. We did not try to reproduce those with MQCT (e.g., by repeating calculations on a fine grid of points) but, from Figs. 1–3 combined it looks like MQCT may be insensitive to narrow scattering resonances.

Figure 4 is presented in order to quantify deviations of MQCT method from the full-quantum benchmark results. In this figure, the percent-errors for quenching cross sections are plotted as a function of the ratio  $E/\Delta E$ , together for all transitions discussed above. The data of Fig. 4(a) indicate that results of *scaled* MQCT rarely deviate from the full quantum results by more than 20%. This performance is rather consistent through the entire range of energies considered here. The

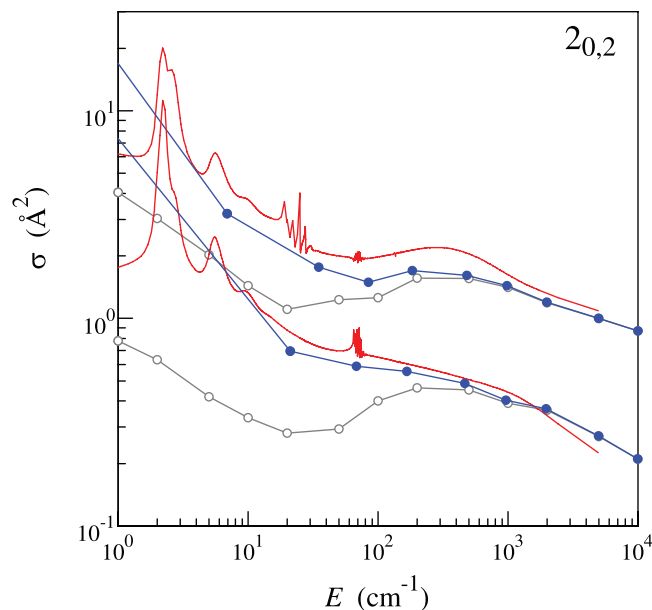


FIG. 3. Same as in Figs. 1 and 2, but for quenching of the second excited state  $2_{0,2}$  of para-water. Three upper curves correspond to transition into the first excited state  $1_{1,1}$ , while three lower curves correspond to transition into the ground state  $0_{0,0}$ .

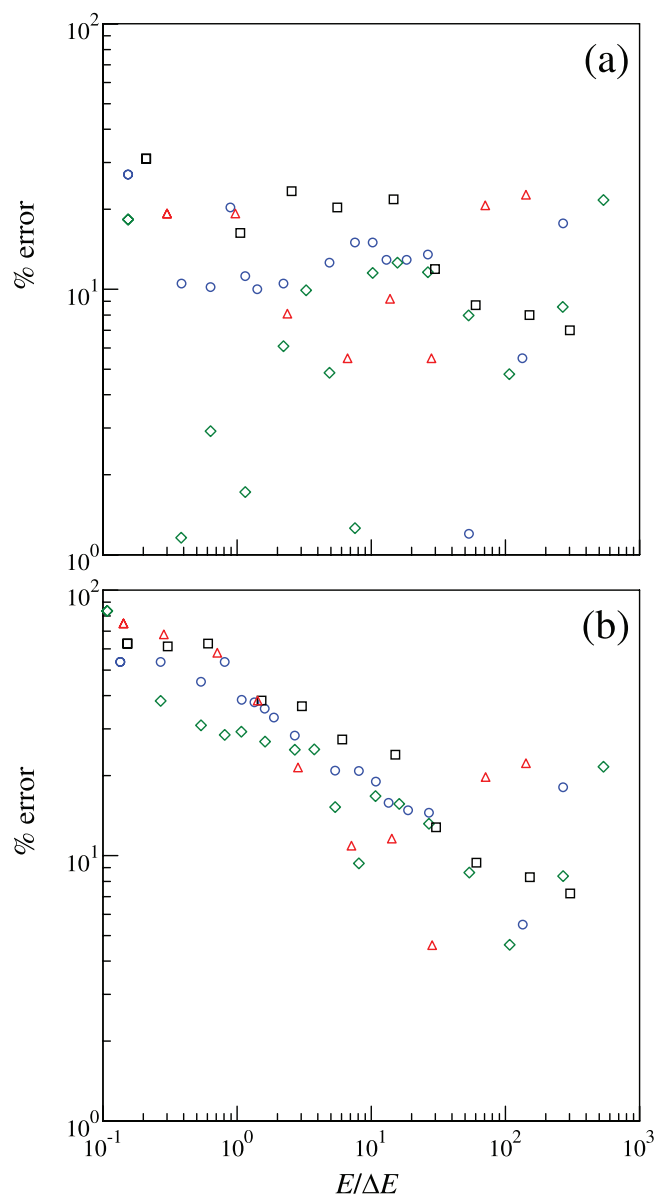


FIG. 4. Percent-errors of all MQCT calculations presented in Figs. 1–3. Frame (a) is for the average-velocity approach (i.e., for the final results), while frame (b) is for the raw MQCT data. Quenching of  $1_{1,1}$  – blue circles, quenching of  $1_{1,0}$  – green diamonds, quenching of  $2_{0,2}$  into  $1_{1,1}$  – black squares, and into  $0_{0,0}$  – red triangles.

average value of error (over all data points of Fig. 4(a)) is less than 13%, which is very encouraging. In Fig. 4(b), we collected the percent errors of the *raw* MQCT results. Here, we better see correlation between the ratio  $E/\Delta E$  and the error of MQCT, but the values of errors are much larger for these *raw* results than for *scaled* results, particularly at lower collision energies, where the errors approach 100%.

## VI. CONCLUSIONS

In this work, we applied the mixed quantum/classical theory to compute quenching cross sections of several rotationally excited states of water molecule by impact of He atom. To our best knowledge, this is the first study where MQCT methodology is applied to a real system of asymmetric top

rotor + atom, in a broad range of collision energies, and results are tested against the full-quantum calculations on the same potential energy surface. The purpose of this study was not really to test the numerical efficiency of the method, and not that much its accuracy, but rather to investigate whether this method carries potential for consistent theoretical treatment of rotationally inelastic transitions in a broad range of scattering energies.

In current implementation of the MQCT method, there are two major sources of errors: One is important at energies below  $10 \text{ cm}^{-1}$ , while the other shows up at energies above  $500 \text{ cm}^{-1}$ . Indeed, it is known that MQCT method becomes less accurate at collision energies below  $\Delta E$ , due to its intrinsic approximations.<sup>19,24,25</sup> This is expected and cannot be avoided, although we saw that employment of the average-velocity principle (scaling of collision energy) in order to satisfy microscopic reversibility<sup>19</sup> helps to improve MQCT results dramatically at low and intermediate energies. In contrast, at higher energies MQCT is expected to be more accurate in principle. The errors we see in this work at higher energies are due to current implementation, rather than due to MQCT assumptions. Namely, in this work we had to cut off the basis set size of MQCT calculations, in order to make them computationally affordable. This deficiency can probably be eliminated, by developing a more efficient version of MQCT (see below). Overall, the errors of MQCT method are within 20% almost everywhere through four-orders-of-magnitude range of collision energies, except near resonances, where the errors are somewhat larger.

Although the mixed quantum/classical theory is easier to formulate in the SF reference frame, we found that numerical calculations in SF are extremely demanding computationally. Namely, the state-to-state transition matrix is complex-valued and is dense,<sup>23</sup> so that summation over its elements in Eqs. (5) and (13) is a costly procedure. Furthermore, each element of the transition matrix depends on three variables, either polar ( $R$ ,  $\Theta$ ,  $\Phi$ ) or Cartesian ( $X$ ,  $Y$ ,  $Z$ ), and these variables change continuously along trajectories. We considered building splines of all these data (each matrix element as a function of three variables), but found that memory requirements would make this approach impractical. Thus, we decided to re-compute matrix elements on the fly, multiple times per time-step, since gradients are also needed for classical equations of motion, Eq. (13). This worked, but was costly in terms of the CPU time and, as a result, our MQCT calculations came out even more expensive than the benchmark full-quantum CC calculations! So, at this point we cannot recommend MQCT as a computationally efficient method yet, but we have all reasons to expect that MQCT will be much more efficient in the BF reference frame. Indeed, in the BF reference frame the state-to-state transition matrix is real-valued, simply structured around its diagonal and is very sparse.<sup>23</sup> Furthermore, each matrix element depends on one variable only – the molecule-atom distance  $R$ .<sup>23</sup> Such matrix elements could be pre-computed once and then splined efficiently, to use during propagation of MQCT trajectories. We plan to undertake such study in the near future.

## ACKNOWLEDGMENTS

This research was supported by the National Science Foundation (NSF) CNIC program, Grant No. 1338885, and by the CNRS national program “Physique et Chimie du Milieu Interstellaire.” This research used resources of the National Energy Research Scientific Computing Center, which is supported by the Office of Science of the (U.S.) Department of Energy (DOE) under Contract No. DE-AC02-05CH11231.

- <sup>1</sup>J. B. Delos, W. R. Thorson, and S. K. Knudson, *Phys. Rev. A* **6**, 709 (1972).
- <sup>2</sup>K. J. McCann and M. R. Flannery, *Chem. Phys. Lett.* **35**, 124 (1975).
- <sup>3</sup>K. J. McCann and M. R. Flannery, *J. Chem. Phys.* **63**, 4695 (1975).
- <sup>4</sup>K. J. McCann and M. R. Flannery, *J. Chem. Phys.* **69**, 5275 (1978).
- <sup>5</sup>G. D. Billing, *Comput. Phys. Rep.* **1**, 239 (1984).
- <sup>6</sup>G. D. Billing, *The Quantum-Classical Theory* (Oxford University Press, 2002).
- <sup>7</sup>G. D. Billing, “Vibration-vibration and vibration-translation energy transfer, including multiquantum transitions, in atom-diatom and diatom-diatom collisions,” in *Topics in Current Physics*, edited by M. Capitelli (Springer-Verlag, Berlin, 1986).
- <sup>8</sup>M. Cacciatore and G. D. Billing, *J. Phys. Chem.* **96**, 217 (1992).
- <sup>9</sup>G. D. Billing and R. E. Kolesnick, *Chem. Phys. Lett.* **200**, 382 (1992).
- <sup>10</sup>C. Coletti and G. D. Billing, *J. Chem. Phys.* **113**, 4869 (2000).
- <sup>11</sup>G. S. Whittier and J. C. Light, *J. Chem. Phys.* **110**, 4280 (1999).
- <sup>12</sup>M. Ivanov and D. Babikov, *J. Chem. Phys.* **134**, 144107 (2011).
- <sup>13</sup>M. Ivanov and D. Babikov, *J. Chem. Phys.* **134**, 174308 (2011).
- <sup>14</sup>M. Ivanov and D. Babikov, *J. Chem. Phys.* **136**, 184304 (2012).
- <sup>15</sup>M. Ivanov and D. Babikov, *Chem. Phys. Lett.* **535**, 173 (2012).
- <sup>16</sup>M. Ivanov and D. Babikov, *Proc. Natl. Acad. Sci. U.S.A.* **110**, 17708 (2013).
- <sup>17</sup>A. Teplukhin, M. Ivanov, and D. Babikov, *J. Chem. Phys.* **139**, 124301 (2013).
- <sup>18</sup>A. Semenov and D. Babikov, *J. Chem. Phys.* **138**, 164110 (2013).
- <sup>19</sup>A. Semenov, M. Ivanov, and D. Babikov, *J. Chem. Phys.* **139**, 074306 (2013).
- <sup>20</sup>G. D. Billing, *J. Chem. Phys.* **57**, 5241 (1972).
- <sup>21</sup>G. D. Billing, *J. Chem. Phys.* **65**, 1 (1976).
- <sup>22</sup>G. D. Billing, *Chem. Phys. Lett.* **50**, 320 (1977).
- <sup>23</sup>A. Semenov and D. Babikov, *J. Chem. Phys.* **139**, 174108 (2013).
- <sup>24</sup>A. Semenov and D. Babikov, *J. Phys. Chem. Lett.* **5**, 275 (2014).
- <sup>25</sup>A. Semenov and D. Babikov, *J. Chem. Phys.* **140**, 044306 (2014).
- <sup>26</sup>B. L. Silver, *Irreducible Tensor Methods: An Introduction for Chemists* (Academic, New York, 1975).
- <sup>27</sup>T. R. Phillips, S. Maluendes, and S. Green, *J. Chem. Phys.* **102**, 6024 (1995).
- <sup>28</sup>A. Messiah, *Quantum Mechanics* (North Holland Publishing Company, 1967), Vol. I.
- <sup>29</sup>K. Patkowski, T. Korona, R. Moszynski, B. Jezierski, and K. Szalewicz, *J. Mol. Struct.: THEOCHEM* **591**, 231 (2002).
- <sup>30</sup>B. H. Yang and P. C. Stancil, *J. Chem. Phys.* **126**, 154306 (2007).
- <sup>31</sup>B. Yang, M. Nagao, W. Satomi, M. Kimura, and P. C. Stancil, *Astrophys. J.* **765**, 77 (2013).
- <sup>32</sup>M.-L. Dubernet, M. H. Alexander, Y. A. Ba, N. Balakrishnan, C. Balana, C. Ceccarelli, J. Cernicharo, F. Daniel, F. Dayou, M. Dornon, F. Dumouchel, A. Faure, N. Feautrier, D. R. Flower, A. Grosjean, P. Halvick, J. Kos, F. Lique, G. C. McBane, S. Marinakis, N. Moreau, R. Moszynski, D. A. Neufeld, E. Roueff, P. Schilke, A. Spielfiedel, P. C. Stancil, T. Stoecklin, J. Tennyson, B. Yang, A.-M. Vasserot, and L. Wiesenfeld, *Astron. Astrophys.* **553**, A50 (2013).
- <sup>33</sup>S. Green, *J. Chem. Phys.* **64**, 3463 (1976).
- <sup>34</sup>J. M. Hutson and S. Green, MOLSCAT computer code, version 14, Collaborative Computational Project No. 6 (Science and Engineering Research Council, United Kingdom, 1994).
- <sup>35</sup>G. McBane, MOLSCAT computer code, parallel version (G. McBane, USA, 2004).
- <sup>36</sup>M. H. Alexander and D. E. Manolopoulos, *J. Chem. Phys.* **86**, 2044 (1987).
- <sup>37</sup>E. Kyro, *J. Mol. Spectrosc.* **88**, 167 (1981).
- <sup>38</sup>S. Green, S. Maluendes, and A. D. McLean, *Astrophys. J. Suppl. Ser.* **85**, 181 (1993).